Determining the effective electromagnetic properties of negative-refractive-index metamaterials from internal fields

Bogdan-Ioan Popa* and Steven A. Cummer
Department of Electrical and Computer Engineering, Duke University, Durham, North Carolina 27708, USA
(Received 10 November 2004; revised manuscript received 21 July 2005; published 4 October 2005)

Effective electromagnetic properties of negative index of refraction metamaterials (NIMs) can be hard to measure. We show through simulations that electromagnetic fields inside a typical, physically realizable wire-SRR (split ring resonator) NIM are more homogeneous than one might expect inside such metamaterials, and sufficiently structured to be useful for interpretation. Specifically, simulations show that the electric field phase is surprisingly smooth inside the NIM, including at the edges of the material, and can thus be used to reliably estimate the effective length of the material, a critical parameter when determining the effective material properties using many methods. The effective length, together with amplitude and phase measurements inside the material, can further be used to measure with good precision and minimum ambiguity the effective material properties of a NIM. To validate this technique, we show that the material properties obtained using it very closely match those derived from *S* parameters. The inherent redundancy in the field data makes this method less sensitive to measurement errors than one based on transmission/reflection measurements, thus making it suitable for simulations and for experiments. We also show that, for experiments, given the periodicity of the NIM, one measurement per cell is generally enough to retrieve with good precision these material properties.

DOI: 10.1103/PhysRevB.72.165102 PACS number(s): 42.25.Bs, 41.20.Jb, 78.20.Ci

I. INTRODUCTION

Since the first metamaterials exhibiting negative index of refraction were built,[1,2] research has focused on determining reliably their electromagnetic properties. Most of the metamaterials analyzed today (in both simulation and experiment) consist of multiple layers of wires and split ring resonators (SRRs). Previous research[3,4] has shown that, if these components are small enough compared to the working wavelength, the material they form can be characterized by effective bulk medium properties such as the index of refraction, n, and relative impedance, $Z=\sqrt{(\mu\varepsilon_0)/(\mu_0\varepsilon)}$, or, equivalently, permittivity, $\varepsilon=\varepsilon_0 n/Z$, and permeability, $\mu=\mu_0 nZ$. The permittivity and permeability of wire-only and SRR-only media, respectively, can be found analytically,[4,5] but when the wires and SRRs are combined in a single medium, the complex interactions between the components of the metamaterial change the values of permittivity and permeability in ways that are difficult to predict.[6] Consequently, effective metamaterial properties are determined in experiments and simulations[2,6] by inferring n and Z indirectly from the reflection and transmission coefficients at the negative index of refraction metamaterial (NIM) boundaries, coefficients that are computed from the external fields. The ambiguities involved when solving for these material properties are, as stated in Ref. 6, important issues when using this method. For example, the equation that gives n has multiple solutions; choosing which one is the correct solution can be difficult, especially for thick samples. The effective length of the NIM, and consequently the effective boundaries of the region that shows the NIM behavior, are another source of ambiguities. This effective length is a parameter in the equations that give n and Z but is not obviously defined in a material composed of macroscopic inclusions. Also, the solution for n and Z is exactly determined by the values of the S_{11} and S_{21} parameters. Thus, without any overdetermination, the retrieved values of n and Z can be sensitive to measurement errors, therefore making this method not always reliable.

In the course of experimentally demonstrating antiparallel energy flow and phase velocities inside a NIM, it was shown in Ref. 9 that internal field measurements can be used to extract the effective permittivity and permeability of the material. However, Ref. 9 showed only one measurement per cell, which is insufficient for a good analysis of the field behavior inside the metamaterial. For a better characterization of the fields, a finer sampling grid is needed. Reference 9 also suggested that the boundaries of the metamaterial were sharp, but it is important to see how sharp they are because this sharpness is directly connected to how accurately one can evaluate the effective thickness of the metamaterial (a source of ambiguities, as we have seen above). Determining how sharp these boundaries are requires subcell field measurements not shown in Ref. 9. Here we investigate these issues, and in doing so we also elucidate the fundamental behavior of electromagnetic fields in wire-SRR metamaterials. We find that the phase inside NIMs is surprisingly smooth, including at the edges of the material, and consequently can be used to reliably determine the effective boundaries, and, implicitly, the effective length of the NIM. We investigate how the internal fields vary with position relative to the metamaterial inclusions and find that there are certain locations where these fields are surprisingly close to what one would expect inside a homogeneous material. When fields are measured in these locations, the effective material boundaries are surprisingly sharp and very close to the outer edge of the last metamaterial inclusion in the slab. Using the effective length of the NIM and the spatial distribution of the electric field inside and outside the NIM, the effective index of refraction and impedance of the metama-

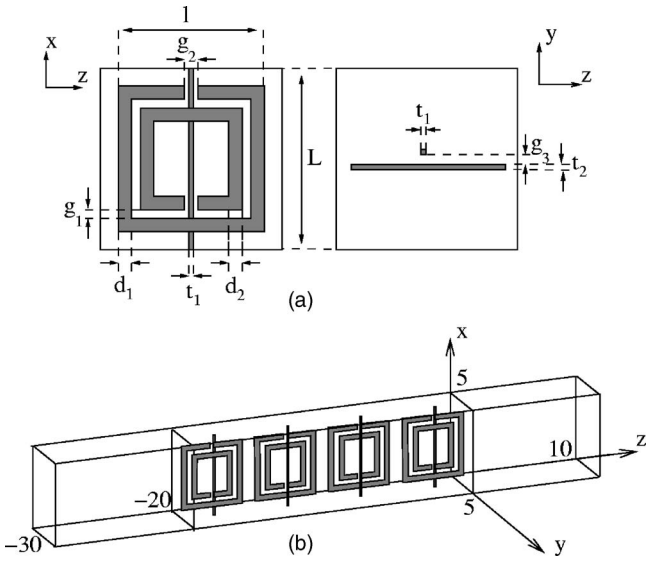

FIG. 1. (a) Unit cell: $L=5$ mm, $l=4$ mm, $d_1=0.33$ mm, $d_2=0.33$ mm, $g_1=0.1$ mm, $g_2=0.3$ mm, $g_3=0.2$ mm, $t_1=0.02$ mm, and $t_2=0.02$ mm; (b) setup: four cells in the propagation direction; PEC boundary conditions on the $x=0$ mm and $x=5$ mm planes; PMC boundary conditions on the $y=0$ mm and $y=5$ mm; wave ports at $z=-30$ mm and $z=10$ mm.

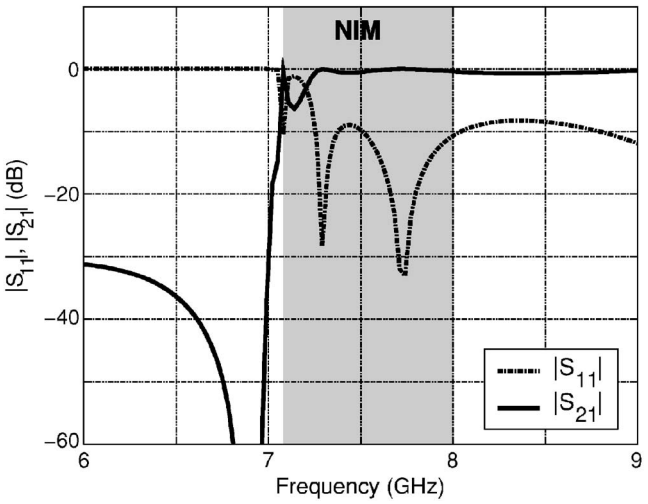

FIG. 2. S parameters.

terial can be determined with minimal ambiguity and good precision by matching the measured internal fields with those computed theoretically for a homogeneous medium, as has been suggested.[9] We evaluate the accuracy of this technique by comparing it to the more traditional S parameters approach, and show that the effective index of refraction and impedance closely match the parameters derived using only S parameters. Moreover, we show that this internal field approach gives a unique solution, in contrast to the potentially ambiguous S parameter technique.

II. SIMULATION PARAMETERS

We used ANSOFT HFSS, a commercial solver of Maxwell's equations, to simulate the electromagnetic fields inside a metamaterial composed of layers of lossless wires and SRRs. The unit cell of this medium, shown in Fig. 1(a), is a cube having 5 mm edges. Using one wire per cell, we obtained, as in Ref. 6, a wire medium that has a lattice constant of 5 mm. Further, we modified the design described in Ref. 2 to obtain an SRR with a resonant frequency near 7 GHz. The electric field is polarized in the direction of the wires, while the magnetic field is perpendicular on the SRRs plane. The complete simulation arrangement, shown in Fig. 1(b), consists of a metamaterial section composed of an array of four unit cells in the propagation direction placed between two regions filled with air. In order to simulate infinite media in the transverse direction, we set the top and bottom boundaries to be perfect electric conductors (PEC), and the side boundaries to be perfect magnetic conductors (PMC). Because of this choice of boundary conditions and the asymmetry of the unit cell, the period of the structure is actually two cells, as opposed to one cell periodicity if using periodic boundary conditions. However, the fundamental properties of the equivalent infinite metamaterial are similar in both cases. The three-slab structure is excited at the $z=-30$ mm end with a plane wave propagating in the $+z$ direction. Initially, HFSS divided the solution domain into about 4000 tetrahedral elements, a mesh that was refined in subsequent steps. The electric field was monitored to determine when convergence was reached. Between the 20th and 24th step, the field distribution remained essentially unchanged. The final mesh computed during step 24 had over 120000 elements. We conclude that the simulation has reliably converged.

A plot of the S parameter magnitudes is shown in Fig. 2. Past S parameter simulations and experimental measurements have usually shown a negative index band surrounded by stop bands where $\mu>0$.[10] This structure differs in that ε becomes positive at the same frequency (8 GHz) that μ becomes positive and thus there is no stop band. S parameter analysis and analysis of the electric field inside the NIM (similar to what we show next) show that the wire-SRR medium described above exhibits negative index of refraction in the 7.1–8.0 GHz band. Below we present such measurements for plane waves propagating at 7.55 GHz (i.e., the middle of the negative index transmission band). Our goal is to simulate spatial fields inside the structure and match them with an analytical solution for a homogeneous medium. This procedure allows us to retrieve the effective electromagnetic parameters, n and Z. As a verification, we compare these values with those derived from the S parameters, as described in Ref. 6.

Given that the unit cell is approximately eight times smaller than the wavelength of the incident wave, it is reasonable to assume that the second region can be approximated as homogeneous with the permittivity and permeability tensors $\bar{\bar{\varepsilon}}$ and $\bar{\bar{\mu}}$, respectively. Assuming a $+j\omega t$ time dependence, the incident plane wave can be written $\vec{E}_i=\hat{x}E_0e^{-jk_0(z+d)}$, where k_0 is the wave number in the air and d is the NIM length. Since the electric field is polarized in the x direction and consequently the magnetic field in the y direction, it follows that the only relevant components of the permittivity and permeability tensors inside the NIM are ε_x

and μ_y. Let the wave vector inside the negative index material be $\vec{k}=\hat{z}k_0 n$. Noting that the SRR orientation means that the structure has no bianisotropic behavior,[8] it is easy to show that the electric field inside the three media is given by[7]

$$\vec{E}_1(z) = \hat{x}E_0\left[e^{-jk_0(z+d)} + \frac{(Z^2-1)(1-e^{-2jk_0nd})}{(Z+1)^2-(Z-1)^2e^{-2jk_0nd}}e^{jk_0(z+d)}\right], \tag{1}$$

$$\vec{E}_2(z) = \hat{x}E_0\frac{2Z(1+Z)e^{-jk_0nd}}{(Z+1)^2-(Z-1)^2e^{-2jk_0nd}}\left(e^{-jk_0nz} + \frac{1-Z}{1+Z}e^{jk_0nz}\right), \tag{2}$$

$$\vec{E}_3(z) = \hat{x}E_0\frac{4Ze^{-jk_0nd}}{(Z+1)^2-(Z-1)^2e^{-2jk_0nd}}e^{-jk_0z}. \tag{3}$$

It follows that the scattering matrix components S_{11} and S_{21} are, respectively,

$$S_{11} = \frac{E_1(-d-a)-E_i(-d-a)}{E_i(-d-a)} = \frac{(Z^2-1)(1-e^{-2jk_0nd})e^{-2jk_0a}}{(Z+1)^2-(Z-1)^2e^{-2jk_0nd}}, \tag{4}$$

$$S_{21} = \frac{E_3(a)}{E_i(-d-a)} = \frac{4Ze^{-jk_0nd}e^{-2jk_0a}}{(Z+1)^2-(Z-1)^2e^{-2jk_0nd}}, \tag{5}$$

where a is the length of each of the regions filled with air.

III. SIMULATED MEASUREMENTS AND MATCHING PROCEDURE

Equations (4) and (5) have already been used by others[1,2] in order to find the effective material parameters n and Z. We will show next how we can find these parameters by matching the fields computed using Eqs. (1)–(3) with those obtained using HFSS. A plot of the simulated fields averaged across the transverse (xy) plane (see the solid line in Fig. 4) shows that the fields inside the metamaterial are not homogeneous, but sufficiently structured to be useful for interpretation. Thus, the averaged phase is surprisingly smooth inside the metamaterial, and can be used to extract the effective thickness of the wire-SRR slab, d, an important parameter that is difficult to determine using other methods. The sharp transition between the positive and negative phase slopes allows us to accurately determine the effective boundaries of the metamaterial. For this thin sample we see that these boundaries coincide with the outer boundaries (not the centers) of the last cells (i.e., $z=-20$ mm and $z=0$ mm), and thus the effective thickness is $d=20$ mm.

On the other hand, the amplitude is more inhomogeneous, because the averaged fields include not only the contribution of the propagating wave that we want to measure, but also the contribution of the intense quasistatic near fields in the proximity of the wires and SRRs (see Fig. 3). Despite these inhomogeneities, we can still match the simulated averaged fields with the theoretical fields to find the effective material parameters. However, while computing field averages is possible in simulations, this approach is not suitable for experiments. From an experimental point of view, it is much easier to sample the fields on a single line parallel to the direction of propagation. If this line is chosen far from the metallic inclusions, where the contribution of the quasistatic fields in the proximity of these inclusions is minimal, then we can measure the fields associated with the propagating wave more accurately, and consequently we can determine the effective material parameters with good precision. For these reasons we measured the fields along the three lines shown in Fig. 4(a). The field distribution along these lines is presented in Fig. 4(b), and shows that the fields are smooth enough to allow the fitting procedure shown next to be performed on any of these three lines. However, as it was observed experimentally for a similar wire-SRR material,[9] and

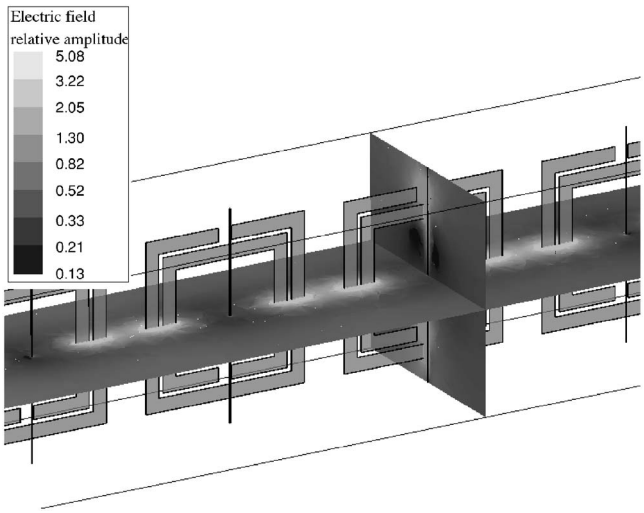

FIG. 3. Amplitude of the electric field inside the slab. The intense fields between adjacent SRRs are responsible for the oscillatory behavior of the fields inside the wire-SRR medium.

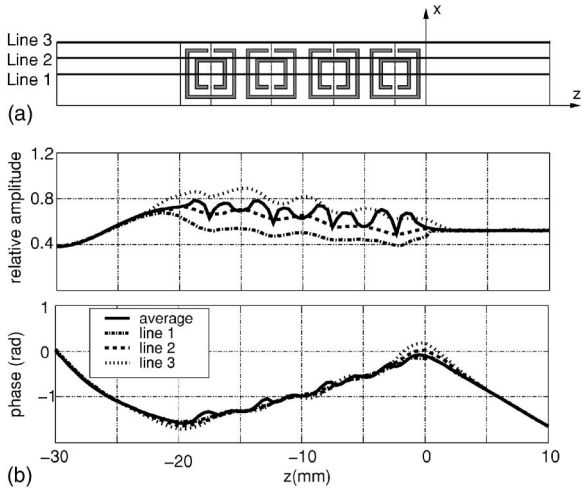

FIG. 4. (a) The electric field is measured along three lines given by the following equations: $x=2.5$ mm, $y=0$ mm (line 1); $x=3.75$ mm, $y=0$ mm (line 2); $x=5$ mm, $y=0$ mm (line 3). (b) Electric field (amplitude and phase) averaged over the transverse xy plane, and the electric field along the three sampling lines.

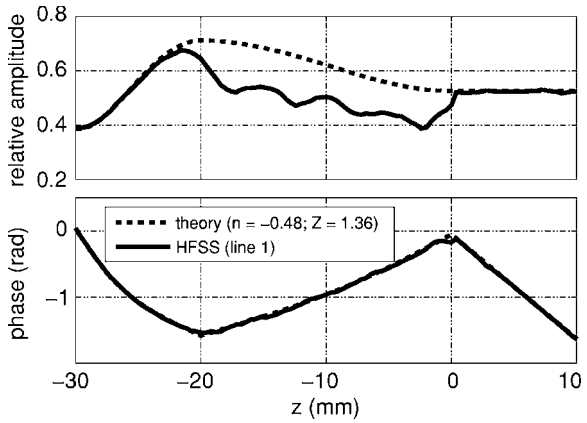

FIG. 5. Result of the curve-fitting procedure for determining n and Z. A good match was obtained for $n=-0.48$ and $Z=1.36$.

as Fig. 4(b) suggests, the possibility of amplitude enhancement or suppression with respect to the theoretical, expected amplitude needs to be accounted for. Since the amplitude outside the wire-SRR slab needs to be matched closely, it can be easily determined whether this shift in amplitude is present or not.

Next we focus on the fields measured along line 1, since this line is the most centered and consequently the phase along it is less oscillatory. The small standing-wave ratio (X_{SWR}), defined as the ratio between the maximum and minimum values of the electric field) in region $z<-20$ mm means that the reflection coefficients at the air-metamaterial boundaries are also small. Consequently, to first order, we can neglect the effects of the reflected wave inside the metamaterial, and thus we can assume $n=-(d\phi/dt)(1/k_0)$, or, using Fig. 4, $n=-0.44$. As a first approximation, we choose $Z=1.5$ to reflect the small standing wave ratio ($X_{\mathrm{SWR}}<2$) and the electric field maxima at $z=-20$ mm. We compare the theoretical plots of the field amplitude and phase from this initial estimate with the simulated fields in Fig. 4, and subsequently iterate the n and Z estimates to obtain theoretical plots that match the measured fields more closely. We find $n=-0.48$ and $Z=1.36$, which indeed give a small standing-wave ratio in region $z<-20$ mm ($X_{\mathrm{SWR}}=1.35$). The good final agreement between the simulated metamaterial fields and homogeneous medium fields is shown in Fig. 5. This agreement shows that there is at least one line along which the phase closely matches the theoretical phase even inside the border cells, as if the metamaterial were continuous even in the proximity of its boundaries. The same fitting procedure was also performed using lines 2 and 3 (not shown), and the recovered effective refractive index and relative impedance were the same as above. Also, as can be seen in Fig. 4 and 5, the smoothness of both phase and amplitude in regions far from the metallic inclusions means that, in experiments, one measurement per cell is generally enough to perform the fitting procedure presented above.

To confirm our ability to measure the effective medium parameters from the internal fields, we compare the values of n and Z determined above with those obtained from inverting Eqs. (4) and (5), as described in Ref. 6. We use the scattering matrix components reported by HFSS as the initial data. Recall that this method gives multiple solutions for n and Z. However, since we know the amplitude and phase distributions inside the structure, we can choose the correct solution. We obtain $n=-0.4797$ and $Z=1.3521+0.0199j$, which matches well the values determined from the curve-fitting procedure.

IV. MEASUREMENT UNIQUENESS

In the previous section, we found one (n,Z) pair for which the corresponding theoretical fields match the simulated fields. It is important to see whether there are other (n,Z) pairs that give the same electric field distribution inside the structure or not. We will show next that the answer is no and, indeed, the internal electric field uniquely determines the (n,Z) pair.

Suppose there are two pairs, (n_1,Z_1) and (n_2,Z_2), that give the same values for $E_1(z)$, $E_2(z)$, and $E_3(z)$ for every value of z. Since z is a variable in the exponentials in Eq. (2), it follows that the arguments and coefficients of the exponentials in Eq. (2) must be the same, that is,

$$k_0 n_1 z = k_0 n_2 z, \tag{6}$$

$$\frac{2Z_1(1+Z_1)e^{-jk_0n_1d}}{(Z_1+1)^2-(Z_1-1)^2e^{-2jk_0n_1d}} = \frac{2Z_2(1+Z_2)e^{-jk_0n_2d}}{(Z_2+1)^2-(Z_2-1)^2e^{-2jk_0n_2d}}, \tag{7}$$

$$\frac{2Z_1(1+Z_1)e^{-jk_0n_1d}}{(Z_1+1)^2-(Z_1-1)^2e^{-2jk_0n_1d}}\frac{1-Z_1}{1+Z_1} = \frac{2Z_2(1+Z_2)e^{-jk_0n_2d}}{(Z_2+1)^2-(Z_2-1)^2e^{-2jk_0n_2d}}\frac{1-Z_2}{1+Z_2}. \tag{8}$$

Equation (6) is equivalent with $n_1=n_2$, while Eqs. (7) and (8) give

$$\frac{1-Z_1}{1+Z_1} = \frac{1-Z_2}{1+Z_2}, \tag{9}$$

which is equivalent with $Z_1=Z_2$. It follows that only one pair (n,Z) gives a certain set of functions $E_1(z)$, $E_2(z)$, $E_3(z)$. In our case, for example, a 10% change in n or Z results in a clear mismatch between the theoretical fields and those simulated using HFSS. Moreover, for reasonable values of Z, for which $(1-Z)/(1+Z)$ is relatively small compared to unity, the refractive index determines the slope of the phase inside the NIM [see Eq. (2)], while Z determines the shape of the amplitude curve.

V. CONCLUSIONS

We have shown that electromagnetic field measurements inside a metamaterial consisting of layers of wires and split ring resonators can be used to extract the effective permittivity and permeability of the metamaterial robustly, with minimal ambiguity, and with good precision. These simulations, demonstrated for simulated fields using HFSS, also clearly show that the effective refractive index of such metamateri-

als becomes negative at certain frequencies through the spatial phase gradient inside the metamaterial.

The inherent redundancy in the spatial fields makes this method less sensitive to measurement errors and consequently suitable for experiments and simulations. However, the characteristics of the fields inside the wire-SRR medium, such as the oscillatory behavior of the phase and amplitude due to the quasistatic near fields found in the proximity of the metallic inclusions, require carefully chosen measurement points. We showed that at a reasonable distance away from the SRRs and wires, the total fields are dominated by the contribution of the propagating wave, and therefore phase measurements in this region can be used to reliably determine the effective length of the NIM. Even though the overall amplitude in this region can be enhanced or suppressed, depending on the exact location where the fields are being measured, the general shape of the amplitude remains essentially the same, and can be used, together with phase measurements, to uniquely determine the effective material properties. In the end we validated our technique by matching the determined effective index of refraction and impedance with those computed using the *S* parameter approach.

In summary, our analysis of the fields inside metamaterials composed of discrete inclusions shows that these fields are closer to those inside a homogeneous material in many different ways than one might anticipate.

*Electronic address: bap7@ee.duke.edu

[1] D. R. Smith, W. J. Padilla, D. C. Vier, S. C. Nemat-Nasser, and S. Schultz, Phys. Rev. Lett. **84**, 4184 (2000).
[2] C. G. Parazzoli, R. B. Greegor, K. Li, B. E. C. Koltenbah, and M. Tanielian, Phys. Rev. Lett. **90**, 107401 (2003).
[3] V. M. Shalaev, Phys. Rep. **272**, 61 (1996).
[4] J. B. Pendry, A. J. Holden, D. J. Robbins, and W. J. Stewart, IEEE Trans. Microwave Theory Tech. **47**, 2075 (1999).
[5] J. B. Pendry, A. J. Holden, W. J. Stewart, and I. Youngs, Phys. Rev. Lett. **76**, 4773 (1996).
[6] D. R. Smith, S. Schultz, P. Markos, and C. M. Soukoulis, Phys. Rev. B **65**, 195104 (2002).
[7] U. S. Inan and A. S. Inan, *Electromagnetic Waves* (Prentice Hall, Englewood Cliffs, NJ, 2000), pp. 142–144.
[8] R. Marques, F. Medina, and R. Rafii-El-Idrissi, Phys. Rev. B **65**, 144440 (2002).
[9] S. A. Cummer and B. I. Popa, Appl. Phys. Lett. **85**, 4564 (2004).
[10] K. Li, S. J. McLean, R. B. Greegor, C. G. Parazzoli, and M. H. Tanielian, Appl. Phys. Lett. **82**, 2535 (2003).